The Performance of Electron Counting Direct Detection in Electron Energy Loss Spectroscopy

Shaobo Cheng[1], Paolo Longo[2], Ray D. Twesten[2] and Gianluigi A. Botton[1,*]

[1.] Canadian Centre for Electron Microscopy and Department of Materials Science and Engineering, McMaster University, Hamilton, Canada.
[2.] Gatan Inc., Pleasanton, CA, USA.
* Corresponding author: gbotton@mcmaster.ca

In recent decades, transmission electron microscopy (TEM), and electron energy loss spectroscopy (EELS) in particular, have seen many advances [1,2]. Meanwhile, direct electron detection has been widely used for imaging beam sensitive materials, including the biomaterials, polymers, etc [3,4]. One would instinctively wonder which improvements would be apparent when direct electron detection (DeD) is used to acquire EELS spectra. Early reports have shown the benefits for EELS in a conventional microscope [5]. Taking advantage of the DeD hardware (Gatan K2 IS), we have systematically studied the performance of the K2 IS for the acquisition of EELS spectra at different accelerating voltages on an FEI Titan 80-300 Cubed TEM equipped with a monochromator and two aberration correctors. We have carried out the experiments with the monochromator excited, in order to understand the behaviors of the K2 IS when optimal energy resolution is needed. Using single crystalline $SrTiO_3$ as model system, the point spread functions, modulation transfer functions, signal-to-noise ratio, detective quantum efficiency of the K2 IS detector have been evaluated.

The EELS acquisition system consists of two detectors installed in a Gatan Quantum Energy Filter: the conventional CCD (US 1000) and K2 IS Summit which can be selected independently from each other. Since two detectors are installed in the same spectrometer, it is easy to control the same experimental conditions (such as beam current, same observation area on specimen). Since the K2 IS provides fast acquisition speed (400 frames/second) and small dynamic range, it is suitable for acquiring core loss spectra. Our initial results show that the K2 IS has overall better performance than the CCD at 200 kV while at 80 kV, the K2 detector still provides much higher signal to noise but exhibits slightly broader broader tails of the zero-loss peak (Figure 1) resulting in sharper and less noisy core loss spectra (Figure 1). This information needs to be accounted for when selecting the optimal detector and operating conditions.

Furthermore, four types of noise sources have been quantitively analyzed, including Fano noise, shot noise, gain noise, read-out noise. The signal-to-noise ratio has been calculated for both CCD and K2 under different acquisition conditions. Moreover, we have characterized the performance of the K2 vs CCD in atomic-resolved imaging for high energy features, such as the Sr $L_{2,3}$ edge, including the energy resolution expected when a large acquisition energy range is needed (Figure 2). The results show the remarkable improvements for weak signals when atomic resolution (hence small currents) is required. Systematic measurements related to: dwell time, energy dispersion, signal to noise, energy range, and detector quantum efficiency at different voltages have been carried out and will be presented.

In summary, using $SrTiO_3$ as a model system, we have the evaluated the performance of K2 and CCD working at different accelerating voltages over a range of acquisition parameters. While providing high acquisition speed, the DeD provides significant advantages for materials science applications such as detecting trace elements or analyzing beam sensitive samples [6].

References:
[1] S. Cheng, et al., Science Advances **4** (2018) eaar4298.

[2] X. Li, et al., Advanced Materials Interfaces 6 (2018), p. 1701246.
[3] X. Li, et al., Nature Methods **10** (2013), p. 584.
[4] Y. Zhu, et al., Nature Materials **16** (2017), p. 532.
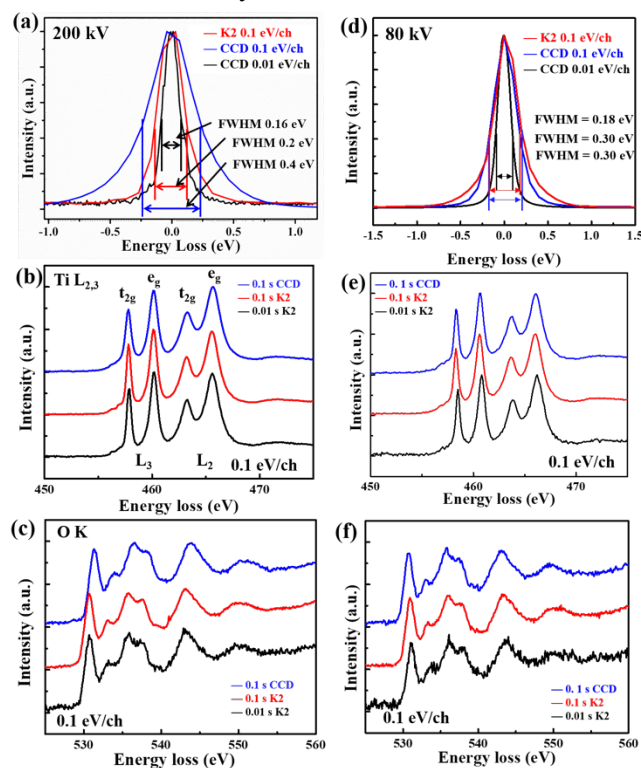[5] J. L. Hart, et al., Scientific Reports **7** (2017), p. 8243.

Figure 1. The EELS spectra acquired on single crystalline $SrTiO_3$ sample. (a) The zero loss peaks (ZLP) acquired by K2 and CCD. The energy resolution for the system is estimated to be 0.16 eV. The full width at half maximum (FWHM) values for K2 and CCD with 0.1 eV/ch dispersion are 0.2 eV and 0.4 eV, respectively. (b) Ti $L_{2,3}$ edges acquired by K2 and CCD with 0.1 eV/ch dispersion. T_{2g} peaks acquired by K2 are narrower than that acquired by CCD. (c) The corresponding EELS spectra for O K edges. Spectra in (a)-(c) were acquired at 200 kV. (d) ZLPs acquired by different detectors with different dispersions under 80 kV. The ZLP acquired by K2 has broader tails. (e)(f) Ti $L_{2,3}$ edges and O K edges acquired with 0.1 eV/ch dispersion under 80 kV.
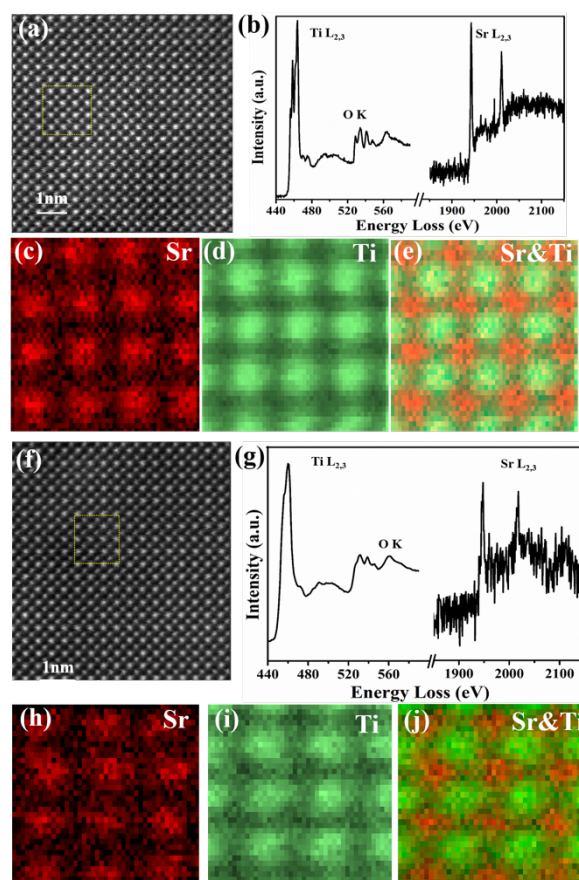

Figure 2. The EELS mapping results for $SrTiO_3$ on the [100] zone axis at 200 kV with 0.1 s/pixel acquisition time. (a) HAADF images for $SrTiO_3$. The area for EELS mapping is marked by yellow rectangle. (b) Ti $L_{2,3}$ edges, O K edge and Sr $L_{2,3}$ edges extracted from K2 EELS mapping result. The e_g/t_{2g} splitting can be seen. (c)-(e) EELS mapping results for Sr and Ti and the combination signal of Sr and Ti. (f) HAADF image acquired before EELS mapping. The yellow rectangle area shows the mapping area for CCD. (g) Ti $L_{2,3}$ edges, O K edge and Sr $L_{2,3}$ edges extracted from the CCD EELS mapping results. More noise can be observed. The e_g and t_{2g} splitting cannot be separated. (h)-(j) Atomic scale mapping results for Sr and Ti and the combination of Sr (red) and Ti (green). The mapping result for Sr $L_{2,3}$ edges is not as clear as that shown in (c) because of the reduced signal-to-noise ratio.